Full paper - 2006 International Joint Topical Meeting: "Sharing Solutions for Emergencies and Hazardous Environments," February 12-15, 2006, Salt Lake City, Utah, USA

# Non-GPS Navigation for Emergency Responders

Lauro Ojeda and Johann Borenstein*
*University of Michigan, 1101 Beal Avenue, Ann Arbor MI, 48109.*
*lojeda@umich.edu, *POC: johannb@umich.edu*

***Abstract*** *- This paper introduces a novel navigation system for walking persons. The system is of particular benefit for emergency responders, who often have to enter and move around in large structures where GPS is unavailable. We refer to our system as "Personal Odometry System" (POS).*

*The POS measures the position of a walking person relative to a known starting position, such as the entrance to a building. This is accomplished by instrumenting one boot of the subject with a 3-axis gyroscope and a 3-axis accelerometer (collectively called "inertial measurement unit" – IMU).*

*This paper describes the POS hardware and explains the basics of our approach. The paper also presents extensive experimental results, which illustrate the utility and practicality of our system.*

## I. INTRODUCTION

This paper describes our Personal Odometry System (POS) for measuring and tracking the momentary location and trajectory of a walking person, even if GPS is not available. We believe that such a system might be of particular value for emergency responders. For example, fire fighters entering a burning building are at risk to be injured and unable to report their position. With the POS reporting the user's position to a central command post, each emergency responder's location could be tracked in real-time. Another application involves the "clearing" of a large building by emergency or security personnel. Their challenge often is to keep track of rooms already cleared and areas that were not cleared, yet. Our system's ability to track each person's location provides a useful solution for this problem.

Our proposed POS does not require GPS. This is an important distinction, since GPS is not available indoors. Furthermore, GPS is unreliable under dense foliage, in so-called "urban canyons," and generally in any environment, in which a clear view of a good part of the sky is not available.

There are some approaches to personal position estimation without GPS. Typically, these systems require external references, also called "fiducials," such as preinstalled active beacons, receivers, or optical retroreflectors. Common to all fiducial-based position estimation systems is that the fiducials must be installed in the work space at precisely surveyed locations before the system can be used. This installation is time consuming and expensive, and in case of emergency response completely unfeasible. Fiducial-based systems also require an active radiation source, such as infrared light [1], ultrasound [2], or magnetic fields [3], which may be undesirable in security-related applications.

Generally, fiducial-based systems perform well and are able to provide absolute position and orientation in real-time. If the application permits the installation of fiducials ahead of time, then these systems have the significant advantage that errors don't grow with time, as is the case in our POS.

Another way of implementing absolute position estimation is computer vision ([4] and [5]). Images are compared and matched against a pre-compiled database. Computer vision has the advantage that the environment does not need to be modified, but the approach requires potentially very large databases. Work is also being done on so-called Simultaneous Location and Mapping (SLAM) methods, which don't require a precompiled database. However, SLAM systems are not as reliable, may accrue errors over time and distance, and poor visibility and unfavorable light conditions can result in completely false position estimation [6][7].

The scientific literature offers only very few approaches that do not require external references. The simplest one of them is the pedometer, that is, a device that counts steps. Pedometers must be calibrated for the stride length of the user and they produce large errors when the user moves in any other way than his or her normal walking pattern. One commercially available personal navigation system based on this principle is the Dead Reckoning Module (DRM) by PointResearch [8]. It uses accelerometers to identify steps, and linear displacement is computed assuming that the step size is constant. Orientation is measured using a digital compass, which is combined with the traveled distance (step counts) to estimate 2-D position. The performance of this system depends on the accuracy of determining the stride

length, which is computed by an initialization procedure using GPS. As is evident, this system is reasonably accurate only if users walk always with the same stride length. Under this condition, the manufacturer reports accuracies up to 5% of the traveled distance. However, the constant stride-length condition cannot be met at all times. For example, emergency responders may run, climb over debris, or may alter their stride length as a function of the weight of their gear.

More sophisticated solutions actually measure the length of every stride in real-time. One such solution using ultrasonic sensors attached to the user's boots is explained in [9]. Ultrasonic sensors require a direct line of "sight" between the boots, which may be a problem on rough terrain. In straight-line walking experiments the authors report an average and maximum error of 1.3% and 5.4%, respectively. Another approach measures the RF phase change between a reference signal located in a waist pack and the one coming from a transmitter located on each boot [10]. A significant drawback of these technologies is that position estimation is restricted to 2-D environments since these systems cannot determine altitude changes and assume that any change is horizontal. Another potential problem is that these technologies use active emissions, which are undesirable for military applications, and they are vulnerable to external interference from the environment or from other units.

## II. Overview

Our proposed POS does not require any external references. Rather, it uses data from a six-Degree-of-Freedom (6-DOF) Inertial Measurement Unit (IMU) sensor attached to the user's boot, as shown in Figure 1.[a] From this data the POS computes the complete trajectory of the boot during each step. On first glance it appears that this approach is destined to fail, since measuring linear displacement using accelerometers is not very feasible. That's because data sampled from accelerometers must be integrated twice to yield linear displacement and this process tends to amplify even the smallest amount of bias drift. However, we developed a practical method that almost completely eliminates this problem – *under certain operational conditions*. We found that such operational conditions exist in legged motion; such as when people walk, run, or even climb. Conversely, our method does not work at all with wheeled, sea-, or airborne motion.

[a)] Note that the currently used IMU is much too large for any practical use. We are using this particular IMU only for the purpose of development in this early stage of our work. A much smaller unit will likely be used when we demonstrate our system at the Judged Robotics Showcase at this conference.

**Figure 1:** BAE SiIMU02 Inertial measurement unit (IMU) mounted to the foot of a walking subject.[a]

Our POS offers these features:

1. Linear displacement (i.e., odometry): This is the most important and most basic function of our system – the measurement of distance traveled, but without measuring the direction. This function works like the odometer of a car, which also does not measure the direction of travel. Our POS performs this function with an error of less than 2% of distance traveled; *regardless of duration or distance*. The POS is also indifferent to the stride length and pace, as well as to the gait, such as walking or running. There is also no need for calibration or fitting our system to the walking pattern of a specific user.
2. Position estimation (i.e., navigation or dead-reckoning): This capability includes odometry as well as the measurement of direction. Position estimation allows our system to determine the subject's actual location in terms of $x$, $y$, and $z$ coordinates, relative to a known starting location. The measurement of direction is based on the use of gyroscopes, which are known to have drift, just as accelerometers do. However, the correction method that we apply to the accelerometers in not effective for gyros. Therefore, our system is currently susceptible to the accumulation of heading errors over time. Our currently used gyros have a quoted bias drift error of 5.0 degrees per hour and, consequently, our POS develops heading errors of this magnitude. Our system also measures vertical position, but less accurately so.

A positioning system with these capabilities can be of great use wherever GPS is denied, including inside buildings, dense forest, tunnels, caves, sewer systems, urban canyons, etc. Emergency responders and security personnel, as well as (eventually) the blind and elderly can benefit from this technology.

Lastly we should note that our POS has a zero-radiation signature, i.e., it does not emit any signals. This makes our system "invisible" to sensors in hostile environments and immune to interference or jamming.

## III. POS HARDWARE

Our current prototype uses a high-quality IMU (see Table I), which is quite expensive and too large to fit in the sole of the boot. Our intention, of course, is to port the system to a smaller IMU later-on in this project.

Our current bulky IMU is strapped to the side of the subject's foot, as was shown in Figure 1. The IMU is connected to an ultra-portable laptop computer through an RS-485 communication port. The IMU is powered using a small external 12-Volt battery, making the whole system portable. The computer runs the Linux operating system patched with a real-time extension and our algorithm runs in real-time.

## IV. POS SOFTWARE

The software for the POS has three modules

- Position estimation module
- Step detection module
- Drift correction module

Each one of these modules will be explained next.

### IV.A. Position Estimation

In this section we give a brief summary of the navigation equations used in our system. For a more detailed explanation see [11].

We follow the convention used in aeronautics for the designation of the navigation and body frames. In mobile robotics the so-called Euler equations are commonly used for attitude representation. However, Euler equations have singularities at ±90° – a limitation that is irrelevant in most ground-based mobile robot applications. However, since in our application the IMU is attached directly to the boot of a walking or running person, tilt angles of 90° or more are possible and likely. For this reason we chose the *Quaternion* representation, which handles any tilt angles.

The Quaternion, $q$, is a vector that defines attitude using four parameters, $a$, $b$, $c$ and $d$. $q$ propagates as a function of the body angular rates, $\omega_b$, according to:

$$\dot{q} = \frac{q \cdot p}{2} \tag{1}$$

where $p = [0, \omega_b]$ and $\omega_b = [\omega_x, \omega_y, \omega_z]$.

Once attitude is computed, the body acceleration, $a_b$, can be computed in terms of the navigation reference frame, $a_n$, using the quaternion vector

$$a_n = q\, a_b\, q^* \tag{2}$$

**Table I:** BAE SiIMU01 characteristics

| Gyroscopes | |
|---|---|
| Range (deg/sec) | ±1,000 |
| Angle Random Walk (deg/rt-hr) | 1.0 |
| Bandwidth (Hz) | 75 |
| Bias drift (deg/hr) | 5.0 |
| **Accelerometers** | |
| Range (g) | ±50 |
| Random Walk (m/s/rt-hr) | 1.0 |
| Bandwidth (Hz) | 75 |

where $q^* = (a - b - c - d)$ is the complex conjugate of $q$.

Velocity, $v_e$, can be computed by integrating the accelerations in the navigation frame after eliminating the local gravity component $g_l$

$$v_n = \int \dot{v}_n\, dt = \int (a_n + g_l)\, dt \tag{3}$$

Finally, position can be computed as the integral of the velocity over time

$$p_n = \int v_n\, dt \tag{4}$$

Note that the navigation equations have been simplified and do not take into consideration the effects of the rotation of the earth on the attitude computation and the Coriolis corrections in the velocity equations. These assumptions are valid in short-term navigation (less than 10 min) but for long-term applications, the use of the full navigation equations becomes necessary.

### IV.B. Dedrifting

Figure 2 shows some of the phases of a stride during normal walking. As is evident from the motion sequence, Point A on the bottom of the sole is in contact with the ground for a short portion of time, $\Delta T$. $\Delta T$ *lasts* roughly from just before *Midstance* ($T_1$= 0.48 sec) to just after *Terminal Stance* ($T_2$ = 0.72 sec) (terminology based on [12]) and is ~0.24 sec in the example here. During that time and unless the sole is slipping on the ground, 'A' is not moving relative to the ground and the velocity vector

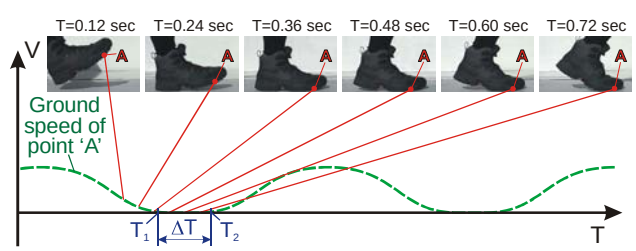


**Figure 2:** Key phases in a stride. During $\Delta T$, all velocities and accelerations of point A in the sole of the boot are zero.

of ‘A’ is $\boldsymbol{V}_A = 0$. The non-slip assumption is warranted because during that phase almost all of the body’s weight rests solely on the area of the sole around ‘A’, thereby increasing traction.

Since the condition $\boldsymbol{V}_A = 0$ is maintained for the significant period of time $\Delta T$ and not just for an instance, we reason that at least sometime during $\Delta T$ the acceleration vector of Point A is also zero. We expect the three accelerometers to show readings of zero during this time. If the reading is not zero, then we assume that the difference between zero and the momentary reading is the result of drift. It is now trivial to record the non-zero value of the accelerometer reading and subtract it from all subsequent readings of the accelerometer. This way we can effectively remove drift from the accelerometer output, at least for a few seconds, until drift continues to change. Luckily, it is the nature of walking or running that the next footstep is just a second away, allowing us to repeat the dedrifting cycle over and over.

The elegance of this approach lies in the fact that in each stride we know at least once the true acceleration of Point A. Our knowledge of the acceleration being zero and the resulting drift correction is always absolute, not relative to the previous correction. Therefore, at least once during every step drift is removed *entirely*. The only accumulation of drift is during the stride. Position errors are thus the result of only a very short period of drift (about one second), before drift is reset to zero.

We use similar reasoning for ground speed, since we know that during $\Delta T$ the true ground speed $\boldsymbol{V}$ is zero. Thus, if the computed velocities obtained using Eq. (3) is different from zero, we reset the computed velocities to the known values, namely, zero. Subsequent computations of velocities use this value of zero as the starting point. The position values remain unaffected during this procedure. The resetting of velocities to zero recurs with every step, during $\Delta T$. This frequent resetting of velocities to the known and absolutely true value of zero assures that any error produced during one step is not carried over to the next ones. For example, if the subject’s foot actually slipped during one step, then the resulting error in velocities exist for just the duration of this one step. Subsequent steps are again error-free. The resulting error in position is just a few centimeters and it remains constant for the remainder of the walk, unless new errors occur.

We call our method, as described up to this point “DEDRIFT-I.” Figure 3 shows the computed velocities during a few strides of a subject walking at walking speed. Note how quickly the uncorrected velocities (interrupted green line) diverge from ground truth, which should be zero in all directions during a period of time during each step.

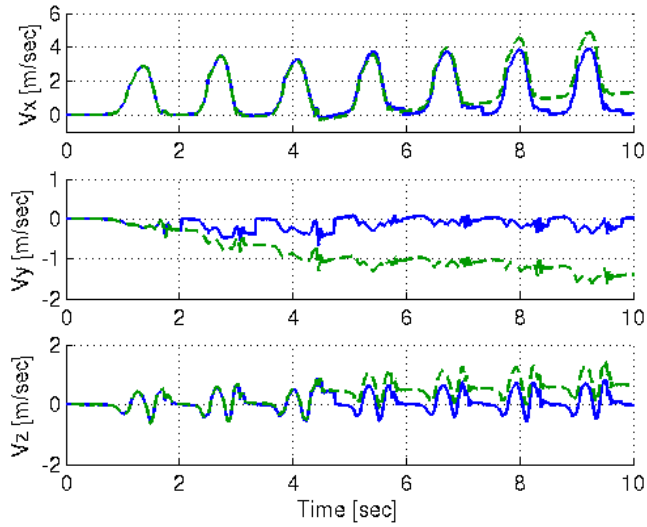


**Figure 3:** Linear velocity of the boot. Dotted green line: without Dedrifting; solid blue line: with Dedrifting. The ‘x’ direction is forward.

We have recently begun the development of an additional and more effective technique, called “DEDRIFT-II.” At the time of writing this paper the DEDRIFT-II method was not mature enough for publication. For this reason we are not including a description of DEDRIFT-II in this paper. However, the experimental results discussed in the following section were all obtained after applying both the DEDRIFT-I ***and*** DEDRIFT-II method.

## IV.C. Step detection

For the “Dedrifting” algorithm to work properly, it is not necessary to identify correctly the exact onset and end of $\Delta T$. Rather, it is sufficient to identify a single instance, $T_s$, within $\Delta T$, in which all accelerations and velocities are zero. In practice, this is not trivial, because the accelerometers suffer from drift, so they never show zero exactly. Experimentally we found that the best indication for $T_s$ can be obtained by observing the three components ($\omega_x$, $\omega_y$, $\omega_z$) of the *angular velocity vector*, $\boldsymbol{\omega}$. During $\Delta T$, the absolute values of these components have a local minimum and their absolute value is small (close to zero). Of course, $\boldsymbol{\omega}$ is directly measured by the three gyroscopes of the IMU, so that data is readily available.

We implement these two empiric rules in our algorithm as follows:

1. The gyro signals, $\omega_b$, are divided in segments of $n = 100$ samples, which correspond to 0.5 sec of data. The exact size of the segment is not critical, but for best results the segment should be short and comparable to the duration of the fastest step. This assures that there is at least one period $\Delta T$ in each segment.

In each segment we compute an array of $n$ = 100 scalars, $\omega_s$. Each element in $\omega_s$ is a scalar representing the amplitude of the $\omega_b$ for that sample.

$$\omega_{s,i} = \sqrt{\omega_{x,i}^2 + \omega_{y,i}^2 + \omega_{z,i}^2} \tag{5}$$

2. Next we determine which elements of $\omega_s$ are smaller than a certain threshold, $\Omega$. We copy all elements that meet this test into a new array, $\omega_T$

$$\omega_{T,i} = \begin{cases} \omega_{s,i} & for \quad \omega_{s,i} < \Omega \\ K & for \quad \omega_{s,i} \geq \Omega \end{cases} \tag{6}$$

where $K$ is some large number. If all elements $\omega_{T,I} = K$, then we conclude that there was no period $\Delta T$ in this segment of $n$ = 100 samples and we investigate the next segment. If there are one or more $\omega_{T,i} \neq K$ in a given segment, then we search for the smallest one and denote the time associated with this sample $T_s$. $T_s$ is the instance at which the locally and absolutely smallest rotation was measured and for our Dedrifting algorithm it signifies the instance, at which all accelerations and velocities of Point A should have been zero.

## V. Experimental Results

In this section we present experimental results aimed at assessing the overall performance of our Personal Odometry System (POS). We tested the POS in a number of scenarios of varying complexity:

- Straight-line experiments.
- Closed loop 2-D experiments.
- Closed loop 3-D experiments.
- Longer-duration experiment.

### V.A. Straight Line Experiments

We performed two sets of experiments with a subject walking along a straight line. In the first set the subject walked at a normal pace of about 1 m/sec. In the second set the subject walked at a brisk pace of about 1.8 m/sec. In both cases the subject stopped at a distance $D$ = 40 m ahead of the starting position.

For each type of experiment we performed $n=5$ runs and we computed the average error, $X_e$, as the average of absolute errors:

$$X_e = \frac{1}{n}\sum_{1}^{n}\left|x_n - D\right| \tag{5}$$

Finally, we expressed the average error as a percentage of travel distance, $E_p$, according to:

$$E_p = 100\frac{X_e}{D} \tag{6}$$

Figure 4 shows the final errors for the 10 runs. Averages of the results of these runs are summarized in Table II. We recall that in this experiment we evaluate the accuracy of our POS in measuring *linear displacement only*. The average errors with the POS are 0.8% and 0.3% of distance traveled for the fast and slow walk, respectively.

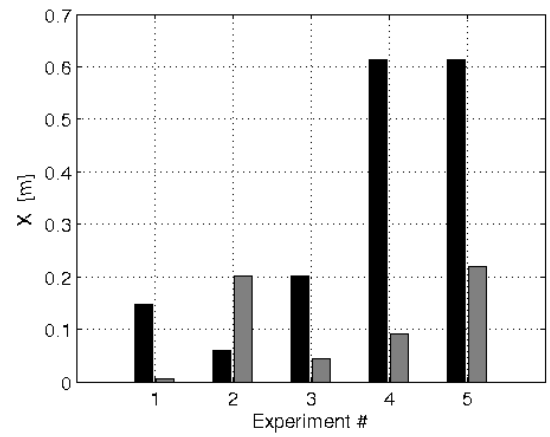


**Figure 4:** Position errors after walking straight ahead for exactly 40 meters. Black: fast walk (1.8 m/sec); gray: slow walk (1.0 m/sec).

**Table II:** Averages of final errors in 10 experiments of walking straight ahead for 40-meters. "Conventional" means conventional dead-reckoning using the IMU, without our Personal Odometry System (POS).

| | Fast Walk | | Slow Walk | |
|---|---|---|---|---|
| | $X_e$ [m] | $E_p$ [%] | $X_e$ [m] | $E_p$ [%] |
| Conventional | 126.1 | 315.2 | 41.25 | 103.1 |
| POS | 0.3 | **0.8** | 0.1 | **0.3** |

### V.B. Closed Loop 2-D Experiments

As explained in Section II, our POS can measure not only distance traveled, but also trajectory and momentary position in X-Y-Z coordinates – relative to a known starting position. The accuracy of the relative position computation depends on the characteristics of the attitude sensors, that is, the gyros. With the high-quality gyros in our current system, walks of up to 15 minutes produce good results. For longer walks or when using lower-quality sensors, a digital compass should be integrated in the navigation algorithm to enhance the heading computation and the performance of the positioning system. However, the results reported in this paper are all from relatively short walks (<15 minutes), using a high-quality IMU and without a compass.

In the closed-loop 2-D experiment, the subject walked along a square-shaped path. Each leg of the square was just over 16 meters in length, resulting in a total path length of $D$ = 65 m. We ran five experiments in clockwise (CW) and five experiments in counter-clockwise (CCW) direction. In all cases the subject walked at the normal walking pace of 1 m/sec.

The absolute return positioning error was computed as

$$e_r = \sqrt{x_r^2 + y_r^2} \tag{7}$$

where

$x_r$ – *return* position error in X-direction.

$y_r$ – *return* position error in Y-direction.

The average error was computed as:

$$E_r = \frac{1}{n}\sum_{1}^{n} e_r \tag{8}$$

The relative error, $E_r$, was expressed as a percentage of total travel distance, $D$

$$E_p = 100\frac{E_r}{D} \tag{9}$$

Figure 5 shows the final position errors for these 10 runs. Averages of the results of these runs are summarized in Table III. The final positioning error in this type of experiments is affected by two sources, the error in the linear displacement estimation and the heading error. Because of the relatively short duration of this walk, the gyros did not contribute much to the final error, and the errors of the linear displacement estimation are small, anyway.

**Table III:** Average of final errors for the square-shaped closed loop path of 65 m total length on horizontal terrain.

| | CW Direction | | CCW Direction | |
|---|---|---|---|---|
| | $E_r$ [m] | $E_p$ [%] | $E_r$ [m] | $E_p$ [%] |
| Conventional | 808.0 | 1,230 | 554 | 851 |
| POS | 0.6 | **0.9** | 0.4 | **0.6** |

## V.C. Closed Loop 3-D Experiments

In the POS, the DEDRIFT corrections are applied to all three components of the velocity vector. Therefore, the POS computes not only the X-Y position, but also the Z-position.

We ran several experiments to assess the accuracy of the POS with regard to position estimation in three dimensions. In these experiments a subject walked along a closed-loop path inside a building included walking up and down two different flights of stairs. Figure 6a shows

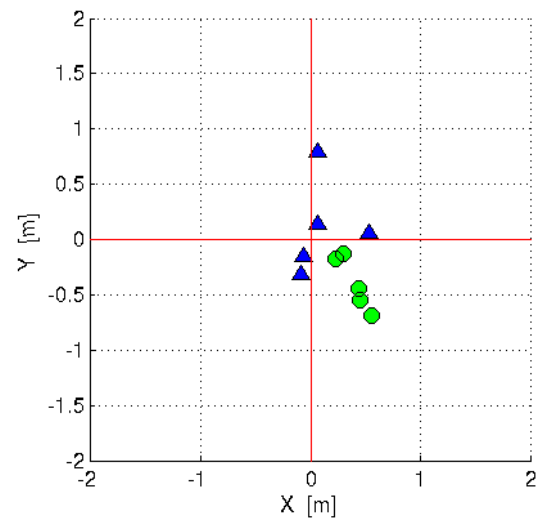


**Figure 5:** Position errors in the vicinity of the target point (0, 0) after walking along the square-shaped closed-loop 2-D path in CW (O) and CCW (Δ) direction.

the 2-D projection of the trajectory for a typical experiment, and Figure 6b shows the 3-D projection.

The approximated total traveled distance was about 104 m. We ran three experiments in CW and three experiments in CCW direction. In all cases the subject walked at the normal walking pace of 1 m/sec.

Figure 7 shows the final position errors for these six runs. Averages of the results of these runs are summarized in Table IV. The final absolute position error, $E_r$, was computed using Eqs. 9 and 10. We took into account only the X- and Y-components of the error, since those are the relevant errors. The percentage error, $E_p$, was computed using Eq. 9. The Z-axis error was computed separately as

$$Z_e = \frac{1}{n}\sum_{1}^{n} |z_r| \tag{10}$$

**Table IV:** Summary of return position errors for the 3-D closed loop path of 104 m total length.

| | CW Direction | | | CCW Direction | | |
|---|---|---|---|---|---|---|
| | $Z_e$ [m] | $E_r$ [m] | $E_p$ [%] | $Z_e$ [m] | $E_r$ [m] | $E_p$ [%] |
| Conventional | 601 | 2,367 | 2,268 | 560 | 2,726 | 2,614 |
| POS | 1.69 | 1.5 | **1.4** | 1.2 | 0.9 | **0.9** |

## V.D. Longer-Duration Experiment

We performed two longer-duration experiments, in which the subject walked for 14 minutes and 12 minutes along mostly horizontal city streets. The travel distances were 1,010 meters and 896 meters, respectively. Figure 8 shows the resulting trajectories and errors, and Table V summarized the results.

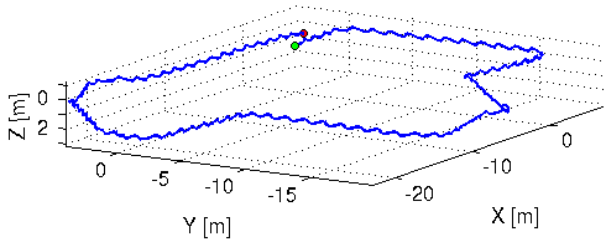


**a**

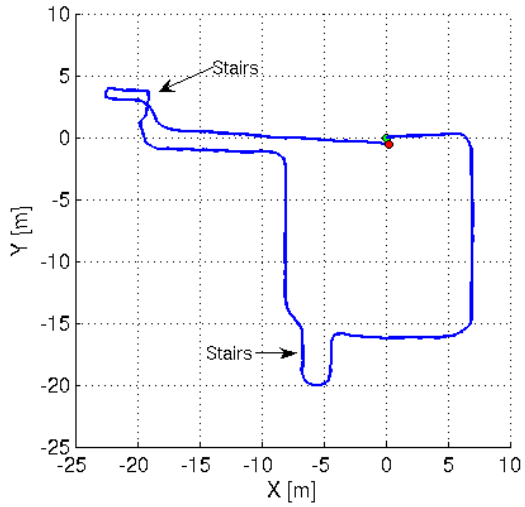


**b**

**Figure 6:** Trajectory of a subject walking along a 3-D closed loop path. (a) 3-D plot; (b) 2-D projection of the same trajectory onto the X-Y plane.

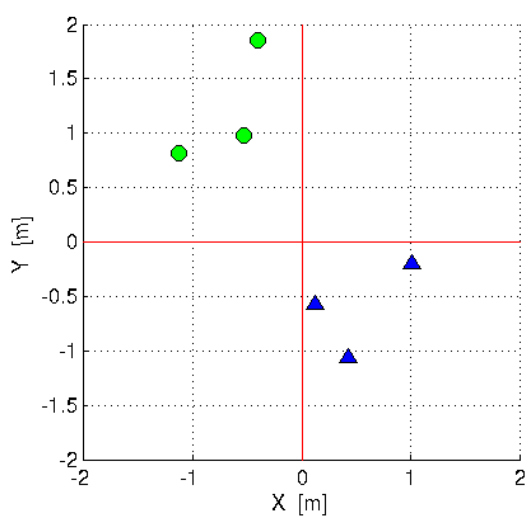


**Figure 7:** Position errors in the vicinity of the target point (0, 0) after walking along a 3-D closed-loop path in either: (O-light color) CW or (Δ-dark color) CCW.

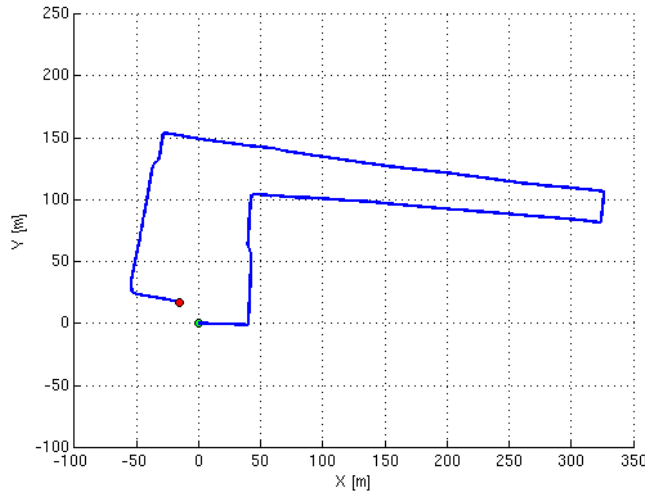


**a**

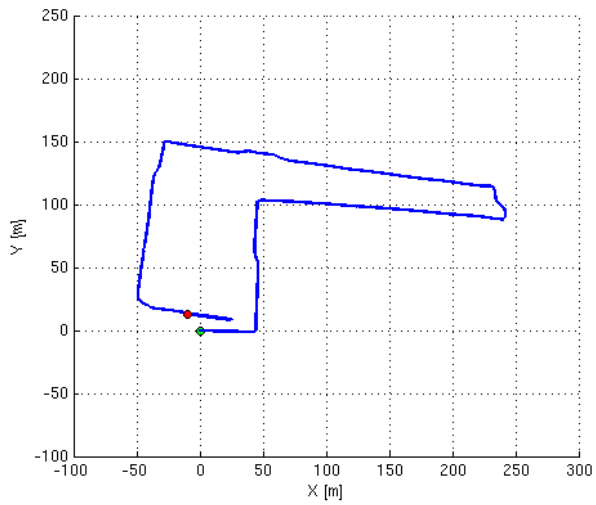


**b**

**Figure 8:** Longer-duration experiments with walks of (a) 14 minutes and (b) 12 minutes.

**Table V:** Summary of results of the longer-duration experiments

| | Duration [minutes] | Distance [m] | Final Pos. Error | |
|---|---|---|---|---|
| | | | Absolute [m] | Relative [%] |
| Walk 1 | 14 | 1,010 | X = -16.0<br>Y = 17.3<br>Z = -19.2 | 2.33% |
| Walk 2 | 12 | 896 | X = -9.6<br>Y = 13.3<br>Z = 9.8 | 1.83% |

## VI. CONCLUSIONS

This paper presented a novel personal odometry system (POS) for emergency responders and security personnel. The POS does not require any external references, such as GPS or other pre-positioned fiducials.

The system is very accurate in measuring linear displacements (i.e., distance traveled, a measure similar to that provided by the odometer of a car) with errors being consistently less than 2% of distance traveled. The POS is also indifferent to pauses or changes in walking gaits. The accuracy of the POS degrades gracefully with extreme modes of legged locomotion, such as running, jumping, and climbing.

In another mode of application, the POS can also measure relative position in terms of X-Y-Z coordinates. Experimental results achieved to date show an accuracy of about 2% of distance traveled in walks up to 10-15 minutes duration. In longer walks the drift of the gyros produces errors that grow without bound as a function of time. We believe that the integration of a compass in our system can help eliminate this problem, although we haven't attempted to do that, yet.

In future work, we will integrate a compass, reduce the size of the POS so that it will fit in the sole of a boot, and perform a variety of improvements to the mathematical algorithms to account for earth rotation and Coriolis acceleration.

Acknowledgements

This work was funded by the Department of the Army via sub-contract No. S-8844-UM-03 administered by General Dynamics Corporation. Funding was also provided by the U.S. Dept. of Energy under Award No. DE FG52 2004NA25587.

## VII. BIBLIOGRAPHY

[1] A. BUTZ, J. BAUS, and A. KRUGER, "Augmenting buildings with infrared information." *Proc. Int'l. Symposium on Augmented Reality, IEEE Computer Society Press*, pp. 93-96, (Oct 5-6, 2000).

[2] J. NEWMAN, D. INGRAM, and A. HOPPER, "Augmented reality in a wide area sentient environment." *Proc. IEEE and ACM Int'l. Symp. on Augmented Reality*, pp. 77-86, (Oct. 29-30, 2001).

[3] Y. LIU, Y. WANG, Y. DAYUAN and Y. ZHOU, "DPSD algorithm for AC magnetic tracking system." *Virtual Environments, Human-Computer Interfaces and Measurement Systems, IEEE Symp. on*, pp. 101-106, (July 12-14 2004).

[4] M. KOUROGI and T. KURATA, "Personal positioning based on walking locomotion analysis with self-contained sensors and a wearable camera." *Proc. Second IEEE and ACM Int. Symp. on Mixed and Augmented Reality*, pp. 103-112, (2003).

[5] H. AOKI, B. SCHIELE, and A. PENTLAND, "Realtime Personal Positioning System for Wearable Computers," *Proc. Int'l Symp. on Wearable Computers*, pp. 37-43, (1999).

[6] C. GALINDO, A. SAFFIOTTI, S. CORADESCHI, P. BUSCHKA, J. FOLKESSON, P., AND H. CHRISTENSEN, "Vision SLAM in the measurement subspace." *Proc. IEEE Int'l Conference on Robotics and Automation*, Barcelona, Spain, April 18-22, (2005).

[7] A. DAVISON, Y. CID, AND N. KITA. "Real-time 3-D SLAM with wide-angle vision". In Intelligent Autonomous Vehicles, Lisboa, Portugal, (Jul. 2004).

[8] T. JUDD, "A Personal Dead Reckoning Module," *Presented at Institute of Navigation's ION 97*, Kansas City, MO, (Sep. 1997).

[9] J. SAARINEN, J. SUOMELA, S. HEIKKILA, M. ELOMAA, and A. HALME, "Personal navigation system'" *Proc. 2004 IEEE/RSJ Int'l Conf. on Intelligent Robots and Systems,* vol. 1, pp. 212-217, (Sept. 28-Oct. 2, 2004).

[10] T. BRAND and R. PHILLIPS, "Foot-to-Foot Range Measurement as an Aid to Personal Navigation." *Institute of Navigation Annual Meeting. 59th*. Albuquerque, NM, (Jun. 23-25, 2003).

[11] D. TTITERTON and J. WESTAON, "Strapdown Inertial Navigation Technology, 2nd Edition." *Progress in Astronautics and Aeronautics Series*, Published by AIAA, 2nd Edition, (2004).

[12] AYYAPPA, E., 1997, "Normal Human Locomotion, Part 1: Basic Concepts and Terminology." *Journal of Prosthetics & Orthotics*, Vo. 9, No. 1, pp. 10-17.